PLOS ONE

RESEARCH ARTICLE

Effects of PTH glandular and external dosing patterns on bone cell activity using a two-state receptor model—Implications for bone disease progression and treatment

Denisa Martonová[1,2]*, Maxence Lavaill[1], Mark R. Forwood[3], Alexander Robling[4], David M. L. Cooper[5], Sigrid Leyendecker[1,2], Peter Pivonka[1]*

1 Mechanical, Medical and Process Engineering, Queensland University of Technology, Brisbane, Queensland, Australia, **2** Institute of Applied Dynamics, Friedrich-Alexander-Universität Erlangen-Nürnberg, Erlangen, Germany, **3** School of Pharmacy and Medical Sciences, Griffith University, Gold Coast, Queensland, Australia, **4** Anatomy, Cell Biology & Physiology, School of Medicine, Indiana University, Indianapolis, Indiana, United States of America, **5** Department of Anatomy, Physiology and Pharmacology, University of Saskatchewan, Saskatoon, Canada

* denisa.martonova@fau.de (DM); peter.pivonka@qut.edu.au (PP)

Citation: Martonová D, Lavaill M, Forwood MR, Robling A, Cooper DML, Leyendecker S, et al. (2023) Effects of PTH glandular and external dosing patterns on bone cell activity using a two-state receptor model—Implications for bone disease progression and treatment. PLoS ONE 18(3): e0283544. https://doi.org/10.1371/journal.pone.0283544

Editor: Mohammadreza Hadizadeh, Central State University, UNITED STATES

Received: October 7, 2022

Accepted: March 10, 2023

Published: March 30, 2023

Data Availability Statement: All relevant data are within the paper and its Supporting information files.

Funding: The work of DM and SL was supported by a fellowship within the IFI programme of the German Academic Exchange Service (DAAD), the Bavarian funding programme BayIntAn and Deutsche Forschungsgemeinschaft (DFG, German Research Foundation) no. 496647562, which are

Abstract

Temporal aspects of ligand specificity have been shown to play a significant role in the case of pulsatile hormone secretion, as exemplified by parathyroid hormone (PTH) binding to its receptor (PTH1R), a G-protein-coupled receptor expressed on surfaces of osteoblasts and osteocytes. The latter binding reaction regulates intracellular signalling and subsequently modulates skeletal homeostasis via bone remodelling. PTH glandular secretion patterns dictate bone cellular activity. In healthy humans, 70% of PTH is secreted in a tonic fashion, whereas 30% is secreted in low-amplitude and high-frequency bursts occurring every 10–20 min, superimposed on the tonic secretion. Changes in the PTH secretion patterns have been associated with various bone diseases. In this paper, we analyse PTH glandular secretion patterns for healthy and pathological states and their link to bone cellular responsiveness (α_R). We utilise a two-state receptor ligand binding model of PTH to PTH1R together with a cellular activity function which is able to distinguish various aspects of the stimulation signal including peak dose, time of ligand exposure, and exposure period. Formulating and solving several constrained optimisation problems, we investigate the potential of pharmacological manipulation of the diseased glandular secretion and via clinical approved external PTH injections to restore healthy bone cellular responsiveness. Based on the mean experimentally reported data, our simulation results indicate cellular responsiveness in healthy subjects is sensitive to the tonic baseline stimulus and it is 28% of the computed maximum responsiveness. Simulation results for pathological cases of glucocorticoid-induced osteoporosis, hyperparathyroidism, initial and steady state hypocalcemia clamp tests indicate α_R values significantly larger than the healthy baseline (1.7, 2.2, 4.9 and 1.9-times, respectively). Manipulation of the pulsatile glandular secretion pattern, while keeping the mean PTH concentration constant, allowed restoration of healthy baseline values from these catabolic bone diseases. Conversely, PTH glandular diseases that led to

gratefully acknowledged. PP and ML would like to gratefully acknowledge funding received through the Australian Research Council (ARC) Industrial Transformation Training Centre for Joint Biomechanics (IC190100020). This work was supported, in part, by a New Frontiers in Research Fund Exploration stream grant (NFRFE-2020-00866) awarded to DMLC and PP.

Competing interests: The authors have declared that no competing interests exist.

maximum bone cellular responsiveness below the healthy baseline value can't be restored to baseline via glandular manipulation. However, external PTH injections allowed restoration of these latter cases.

1 Introduction

Calcium is the most abundant mineral in all vertebrates [1]. Most of the body's calcium (99%) is stored in the bones and teeth, with only 1% stored in blood and other tissues. Calcium serves as a critical regulator of multiple physiological processes, including blood coagulation, nerve conduction, membrane permeability, muscle contraction, enzyme activity and hormone release [2]. Therefore, maintenance of extracellular fluid (ECF) free calcium concentrations in the normal physiological range is tightly regulated in all organisms [3].

As outlined in the recent review by Hernandez-Castellano et al. [1], the classic calciotropic hormones—parathyroid hormone (PTH), calcitriol and calcitonin—regulate calcium homeostasis under normal physiological conditions in mammals by coordinating the availability of ECF free calcium in the blood at the level of the bones, intestine and kidneys. In humans ECF free calcium is regulated by dynamic secretion of PTH by the parathyroid gland and to a lesser contribution from calcitriol and calcitonin [4].

In the following, we focus on PTH secretion patterns of the human parathyroid gland which targets the parathyroid hormone/parathyroid hormone-related protein receptor (PTH/PTHrP type 1 receptor), also commonly known as PTH1R. As highlighted in the review of Cheloha et al. [5], PTH1R is a G-protein-coupled receptor (GPCR) that regulates skeletal development, bone turnover and mineral homeostasis. PTH1R transduces stimuli from PTH and PTH-related-peptide (PTHrP) into the interior of target cells (i.e. cells of the osteoblastic lineage) to promote several divergent signalling cascades. This receptor is able to exist in at least 2 distinct conformation states (R0 and RG) that differ in their signalling response [6]. Ligands that bind selectively to the RG state result in a shorter signalling response, whereas ligands that bind selectively to the R0 state result in prolonged signalling response [7]. The downstream cyclic adenosine monophosphate (cAMP) signalling response is considered to be the primary signalling cascade that mediates the effect of the PTH receptor. PTH1R can modulate a ligand's biological activity depending of the preferential binding to either state [7]. Since most PTH analogues have some affinity for both states of the PTH/PTHrP receptor, the behaviour of a given PTH vis à vis duration of effect is determined by the ratio of binding affinities to each of these receptor states.

As reviewed by Chiavistelli et al. [8], PTH secretion is characterised by an ultradian rhythm with tonic and pulsatile components. In healthy subjects, the majority of PTH is secreted in a tonic fashion (70%), whereas approximately 30% is secreted in low-amplitude and high-frequency bursts occurring every 10–20 min, superimposed on the tonic secretion. Changes in the ultradian PTH secretion pattern have been associated with various diseases including primary and secondary osteoporosis, and hyperparathyroidism. Depending on the dual modifications of pulsatile and tonic components the latter diseases may have different severity of skeletal complications. Furthermore, the pulsatile component can be selectively activated as part of the PTH glandular immediate response to changes in ECF free calcium concentrations [9]. Acute hypocalcemia induces a selective, several-fold increase in bursts frequency and amplitude, whereas hypercalcemia suppresses the PTH pulsatile secretion component, as does prolonged calcitriol therapy.

In the mid 80's, the development of mathematical tools such as heuristic pulse detection methods including Pulsar [10], Cluster [11] and the algorithm of Santen and Bardin [12], allowing decomposition of hormonal release patterns into tonic and pulsatile components, has paved the way for identifying the biological importance of dynamic hormonal secretion. Current theory suggests that biological information in hormonal systems is encoded as a dynamic hormone concentration in the circulating blood. Variations of the concentration are determined by glandular secretion rate and hormonal metabolism. It is now well established that most hormones exhibit a dynamic pattern of episodic secretory and metabolic events. Furthermore, cell biology experiments suggest that pulsatile secretory patterns govern most appropriately the dynamic modulation of the hormone-receptor-interaction, namely receptor de- and resensitisation.

Endocrine diseases are typically defined by comparing serum levels of endocrine factors with the 'normal (or reference) range'. This reference range is used to discern hyper- and hypofunction of respective glands. Dynamic diseases evolve within the normal range and are characterised by increased or decreased secretory dynamics [8]. These high or low dynamic functional states govern cellular responses at the target organs and a disturbed function of a gland can lead to development of progressive diseases. Development of skeletal diseases such as osteoporosis might be linked to the PTH1R signalling pathway and, consequently, it is crucial to understand the dynamics of PTH-PTH1R binding and subsequent signal transduction. Furthermore, osteoporosis therapies such as intermittent PTH(1–34) can also be targeted to PTH1R signalling inducing an osteoanabolic effect [13].

In this paper we utilise a two-state receptor model of PTH-PTH1R originally proposed in [14]. This model is an extension of the work of Potter et al. [15] with respect of introducing a (osteoblastic) *cellular responsiveness* function which is able to distinguish different dynamic PTH dosing patterns. The *cellular responsiveness* has been originally proposed by Li and Goldbeter for pulsatile (square-wave) stimuli [16] applied to gonadotropin-releasing hormone. Using the experimental data of Harms et al. [17, 18] of PTH glandular secretion patterns, we first investigate the reference range of cellular activity representing normal bone homeostasis. We then introduce perturbations of both the tonic and pulsatile components of PTH secretion to mimic various disease states including osteoporosis and hyperparathyroidism. To assess the possibility to achieve a certain *cellular responsiveness* for a given dynamic PTH dosing pattern, we solve a constrained optimisation problem, where the area under the curve (AUC) representing the evolution of the PTH concentration in time (i.e. the mean PTH concentration) is kept constant. These simulations are motivated by the fact that drugs that target calcium-sensing receptors on parathyroid cells can directly affect PTH glandular secretion patterns [19, 20].

In a subsequent analysis, we investigate the effects of an external PTH dose in the form of a subcutaneous (sc) injection on the *cellular responsiveness* for a given disease state. The latter simulations are motivated by the fact that intermittent PTH sc daily injections are used for osteoporosis treatment. The additional PTH dose contributes to an additional *cellular responsiveness* and so has the ability to modify bone cellular activity. We first use the currently clinically approved dose of 20μg daily PTH injections and subsequently, we optimise the dosing pattern to obtain firstly, the maximal *cellular responsiveness* and secondly, the *cellular responsiveness* of a healthy person.

In contrast to previous works [14, 16] presenting an analytical solution for a special case of the optimisation of the *cellular responsiveness*, we make use of numerical approximation methods. The numerical approach is much more flexible in the sense that there are no special case restrictions on the parameters in the model and one can easily consider different scenarios by formulation constrained optimisation problems with various objective functions and constraints.

In Section 2, we introduce the two-state receptor ligand binding model for PTH. This section includes an introduction of various theoretical measures of bone cellular activity (Subsection 2.1) and a representation of PTH plasma concentration (Subsection 2.2). In Section 3, the considered optimisation problems are introduced. In Sections 4 and 5, the results are presented and discussed.

2 Two-state receptor ligand binding model for PTH

Receptor kinetics models have been developed for many different receptor systems, ranging from general models for entire classes of receptors to specific models for a particular receptor expressed in a specific type of cell (see [21, 22] for reviews of existing models). GPCRs such as the PTH1R, are known to exist in various conformations that have different affinities for processes such as binding, activation, and phosphorylation [23, 24]. It has been shown that PTH1R undergoes multiple conformational changes as it binds to ligands and becomes activated [25, 26]. Most commonly, these multiple conformational states can be conceptually grouped into two functional states: active and inactive. A widely accepted model for the activation of GPCRs is the two-state receptor ligand binding model first proposed by Segel et al. in the study of exact sensory adaptation [14]. This model was subsequently employed by Li and Goldbeter to study frequency specificity in intercellular communication [16] and further discussed in [27].

Based on the ability of PTH1R to change conformation independent of a ligand, it is assumed that the two receptor conformational states can transform into each other regardless of its binding to its ligand. This can be achieved either through covalent modification of PTH1R or through simple conformational change. In either case, these correspond to active (or nondesensitised) receptor states, R_a, and inactive (or desensitised) receptor states, R_i, which differ by their capability of eliciting a cellular response upon binding of the ligand. Both receptor states combine with the PTH ligand L to form active and inactive ligand-receptor complexes C_a and C_i (see Fig 1 for a schematic of the model kinetics). This creates a distribution among the four receptor species with the total concentration of receptor $R_T(= [R_a] + [C_a] + [C_i] + [R_i])$.

The ordinary differential equations (ODEs) for the two-state receptor model can be summarised in matrix notation as [14]:

$$\frac{d\mathbf{C}}{dt} = \mathbf{K}(L(t))\mathbf{C}(t), \tag{1}$$

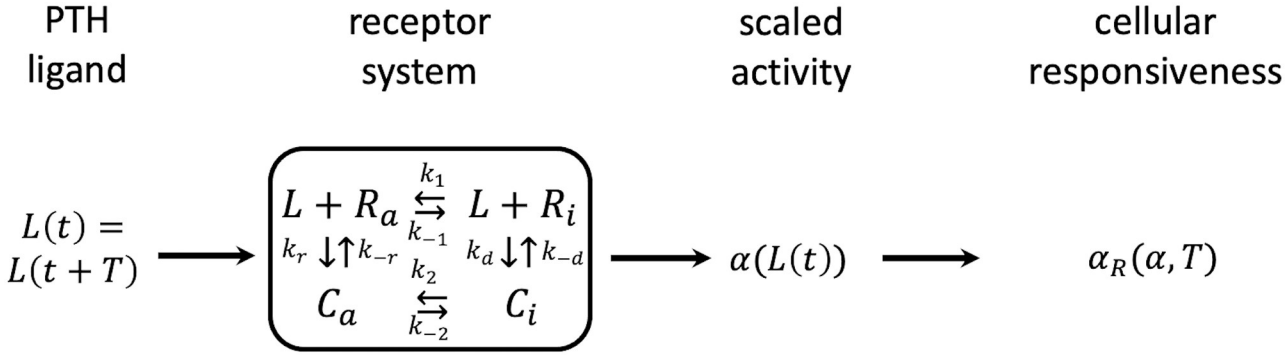

Fig 1. Schematic of the two-state receptor model representing PTH to PTH1R binding based on [16]. $L(t)$ = PTH concentration; t = time; T = period; R_a = active receptor concentration; R_i = inactive receptor concentration; C_a = active ligand-receptor complex concentration, C_i = inactive ligand-receptor complex concentration, $k_{\pm i}$ = kinematic parameters ($i \in \{1, 2, d, r\}$); α = scaled activity; α_R = *cellular responsivenes*.

https://doi.org/10.1371/journal.pone.0283544.g001

where the vector of unknown time-dependent concentration C(t) for the receptor states is given in its scaled form as

$$\mathbf{C} = \begin{bmatrix} r_a \\ c_a \\ c_i \\ r_i \end{bmatrix}, \tag{2}$$

with $r_a = R_a/R_T$, $c_a = C_a/R_T$, $c_i = C_i/R_T$, and $r_i = R_i/R_T$. The constant coefficient matrix describing the ligand-receptor binding kinetics is given as

$$\mathbf{K}(L) = \begin{bmatrix} -k_1 - k_r L & k_{-r} & 0 & k_{-1} \\ k_r L & -k_2 - k_{-r} & k_{-2} & 0 \\ 0 & k_2 & -k_{-2} - k_{-d} & k_d L \\ k_1 & 0 & k_{-d} & -k_{-1} - k_d L \end{bmatrix} \tag{3}$$

see Table 1 for details on the specific parameters. As the above coefficient matrix has not full rank, the system of ODEs reduces to

$$\begin{bmatrix} \dot{r}_a \\ \dot{c}_a \\ \dot{c}_i \end{bmatrix} = \begin{bmatrix} -k_1 - k_r L & k_{-r} & 0 & k_{-1} \\ k_r L & -k_2 - k_{-r} & k_{-2} & 0 \\ 0 & k_2 & -k_{-2} - k_{-d} & k_d L \end{bmatrix} \begin{bmatrix} r_a \\ c_a \\ c_i \\ 1 - (r_a + c_a + c_i) \end{bmatrix} \tag{4}$$

with the conservation condition

$$r_a + c_a + c_i + r_i = 1 \tag{5}$$

being automatically fullfilled by solution of Eq 1. In Eqs (3) and (4), L denotes the ligand concentration, i.e. PTH in plasma (or bone fluid) which binds to PTH1R expressed on osteoblastic cells. We note that, unlike in the paper of [15], we do not compute the PTH concentration from an additional ODE. We assume that this can be approximated by a simple square-wave stimulus characterised by the the peak ligand concentration γ_1, duration of the on-phase τ_1 and period T, see [16]. For the physiological gland pulses, these quantities are derived from experimental data, whereas for the PTH injection, we compute the PTH concentration in plasma from a one compartment pharmacokinetic (PK) model of PTH sc injection in humans

Table 1. Parameter values for the two-state receptor model of PTH-PTH1R as illustrated in Fig 1.

Parameter	Rate constant description	Value	Source
k_1	conversion receptors: $R_a \to R_i$	0.012 min^{-1}	[31]
k_{-1}	conversion receptors: $R_i \to R_a$	0.104 min^{-1}	[31]
k_2	conversion complexes: $C_a \to C_i$	0.222 min^{-1}	[31]
k_{-2}	conversion complexes: $C_i \to C_a$	0.055 min^{-1}	[31]
$K_r = k_{-r}/k_r$	dissociation constant for active complex	1 nM	[29, 30]
$K_d = k_{-d}/k_d$	dissociation constant for inactive complex	10^3 nM	condition of detailed balance [16]

https://doi.org/10.1371/journal.pone.0283544.t001

[28]. This model delivers the periodic ligand stimulus, $L(t) = L(t + T)$. Binding of the ligand to the respective receptor induces a cellular response. As was pointed out by Segel and co-workers [14], the nature of this response as well as the precise manner by which it is linked to ligand binding differ from one particular system to another. In the context of PTH binding to its receptor, PTH1R, the dissociation constant is approximately 1nM [15, 29, 30]. For the kinetic parameters k_1, k_{-1}, k_2, k_{-2}, we adopted the experimentally derived parameters published by [31] for cAMP signalling which uses a GPCR, too. Table 1 summarises the model parameters used for the two-state receptor model.

2.1 Definition of bone cellular responses: Activity functions

Bone cellular response is induced by binding of PTH to PTH1R. Following the work of Segel et al. [14], we assume that the effect induced by the PTH stimulus is measured by a quantity, the so-called scaled activity α, which can be defined as a weighted linear combination of receptors and complexes normalised concentrations as [14]:

$$\alpha(L) = a_1 r_a + a_2 c_a + a_3 c_i + a_4 r_i, \tag{6}$$

where a_i can be viewed as association constants and are hence non-negative [14]:

$$a_i \geq 0, \quad i = 1, 2, 3, 4 \tag{7}$$

The activity defined in Eq (6) should be regarded as a loose measure of how strongly ligand binding to the receptor is contributing to the induction of a physiological cell response.

The choice of affinity coefficients (a_i) is not arbitrary, but based on a particular biological system response. Here, we utilise the *exact adaptation* response defined by Segel et al. [14] as the systems response to a constant stimulus. For the case of *exact adaptation*, the scaled activity α returns to the same value at steady state regardless of the concentration of constant stimulus. The coefficients a_1, a_3 and a_4 are chosen according to [16] with the scaling factor $s = 100$ due to smaller concentration of PTH compared to that work. a_2 is computed such that the exact adaptation condition is satisfied, i.e. $a_2 = ((a_1K_1 + a_4)/(K_1 + 1)(K_2 + 1) - a_3)/K_2$ with $K_1 = k_{-1}/k_1$ and $K_2 = k_{-2}/k_2$ [14].

2.1.1 Dose-response curves for periodic stimuli. As discussed in detail in [16], the aim is to define a meaningful measure of activity for the long-term effect of periodic stimuli. Implicitly, we assume that the cell response can be linked to this quantity. Here, we consider the case of *exact adaptation* for which the steady state value of activity (α_s) equals the basal activity value (α_0). Under these conditions, the basal activity α_0 provides a unique reference value.

2.2.2 Cellular responsiveness. As pointed out in [16], the definition of *cellular responsiveness* is incomplete in terms of the integrated activity $\alpha_T := \int_0^T (\alpha(t) - \alpha_0)dt$ from a physiological point of view. *Cellular responsiveness* should take into account the magnitude of integrated activity as well as the number of activity pulses in a given time interval. Li et al. [16] define the *cellular responsiveness* as the product of two terms:

$$\alpha_R = \frac{\alpha_T}{\alpha_{T_{step}}} \frac{\alpha_T}{T} \tag{8}$$

where $\alpha_{T_{step}}$ is defined as the integrated activity in response to a corresponding step increase in ligand from γ_0 to γ_1:

$$\alpha_{T_{step}}(\gamma_0, \gamma_1) = \tau_a(\gamma_1)\alpha_{M_{step}}(\gamma_0, \gamma_1) \tag{9}$$

In Eq (9), $\alpha_{M_{step}}$ denotes the maximum activity in response to a step increase in ligand from γ_0

to γ_1, while $\tau_a(\gamma_1)$ denotes the adaptation time to a constant stimulus γ_1. The first term in Eq (8) is related to the magnitude of the integrated activity, i.e. $\alpha_T/\alpha_{T_{step}}$, which scales the integrated activity during one pulse of the periodic stimulus with respect to the integrated activity corresponding to a step increase in ligand of the same amplitude. Note $\alpha_{T_{step}} \gg \alpha_T$. The second term is the period (or intrinsic) average of the integrated activity α_T/T, which takes not only the on-phase τ_1, but also the off-phase τ_0 into account. As noted in [16], the latter quantity will equate to a total integrated activity $n\alpha_T$ over a certain time interval $t = nT$.

2.2 PTH ligand concentration in plasma

We note the subscript and superscript *gl* refers to quantities connected to PTH gland secretion.

2.2.1 Physiological parathyroid gland secretion. In humans, plasma PTH fluctuates periodically at a frequency of 3–7 bursts per hour, see S1 Table. Approximately 30% of circulating PTH results from pulsatile secretion and the remaining 70% from tonic secretion [32–34]. The plasma PTH concentration in the latter studies is approximated by a convolution model [35]. In the present study, however, we follow the simplified approach from [14, 16] in which the plasma ligand concentration L_{gl} is approximated by a square-wave stimulus as

$$L_{gl}(\tau_1, T, \gamma_0, \gamma_1, t) = \begin{cases} \gamma_1 & \text{if} \quad (n-1)T \le t \le (n-1)T + \tau_1 \\ \gamma_0 & \text{if} \quad (n-1)T + \tau_1 \le t \le (n-1)T + \tau_1 + \tau_0 \end{cases} \tag{10}$$

where $n = 1, 2, 3, \ldots, N$ represent successive pulses in the repetitive square-wave stimulation. τ_0 and τ_1 denote the off- and on-phase of the signal respectively, while the period T is defined as $T = \tau_0 + \tau_1$, see Fig 2. We note that as the equation system Eq (1) is solved numerically, in contrast to the original work [14], there is no need to introduce dimensionless signal function. Hence, γ_1 and γ_0 denote the concentrations (in pM/L) of PTH in plasma. Further, the model

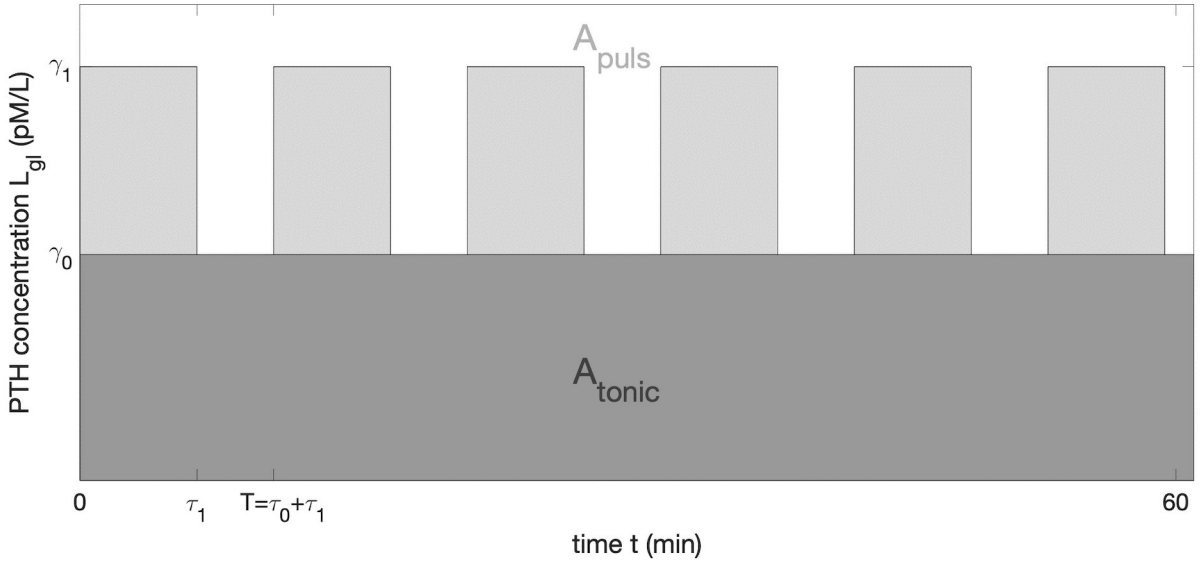

Fig 2. Schematic representation of the square-wave PTH ligand concentration L_{gl} (in plasma) vs. time. γ_1 is the peak PTH concentration due to pulsatile glandular secretion, γ_0 is the PTH concentration due to tonic glandular secretion, and τ_0 and τ_1 are the off- and on-phases of pulsatile component. Dark grey area A_{tonic} represents the plasma concentration resulting from a tonic secretion whereas the light grey area A_{puls} represents the plasma concentration resulting from the pulsatile secretion.

https://doi.org/10.1371/journal.pone.0283544.g002

for the ligand concentration is not restricted to a square-wave stimulus and more complex functions can be used. In order to conserve the dose input signal [36], commonly referred to as AUC, we introduce the integrated concentration per an arbitrary time interval [0, s] as

$$A = A_{tonic} + A_{puls} = \int_0^s L_{gl}(\tau_1, T, \gamma_0, \gamma_1, t)\ \mathrm{d}t, \tag{11}$$

where A_{tonic} and A_{puls} are the AUC of the tonic and pulsatile secretions of PTH, respectively and their ratio is given as $r = \frac{A_{puls}}{A}$.

The mean plasma concentration is assumed to be $\bar{L}_{gl} = 1/T \int_0^T L_{gl}(t)\mathrm{d}t$. As the quantity of our interest is the plasma PTH concentration, see Eq (1), in the subsequent numerical examples, the experimental data from [17, 18] are used, see S1 Table. In these studies, the total plasma concentration was measured.

2.2.2 Additional drug administration. We note the subscript and superscript *inj* refers to quantities connected to an external sc PTH injection. An additional time-dependent PTH dose $D(t)$ can be added in form of a sc injection. To model the resulting plasma concentration, we follow the approach taken by Pivonka and co-workers, i.e. we use a one-compartment PK model of PTH [28, 37] which is given by two ODEs

$$\frac{\mathrm{d}D}{\mathrm{d}t} = -k_a F D(t) \quad \text{and} \quad \frac{\mathrm{d}L_{inj}^{PK}}{\mathrm{d}t} = F V_d k_a D(t) - k_e L_{inj}^{PK}(t), \tag{12}$$

where L_{inj}^{PK} is the ligand plasma concentration, the absorption rate constant k_a represents the drug absorption process from the sc site of injection into the blood stream, and the elimination rate constant k_e represents the drug elimination process from blood, V_d is the distribution volume and F is the bioavailability. Fig 3 shows PTH plasma concentration for the non-linear case and the simplified square-wave stimulus.

Assuming that the peak PTH drug concentration is the same for the square-wave stimulus and the PK model and assuming that the AUC in the (L, t)-plots representing the integrated

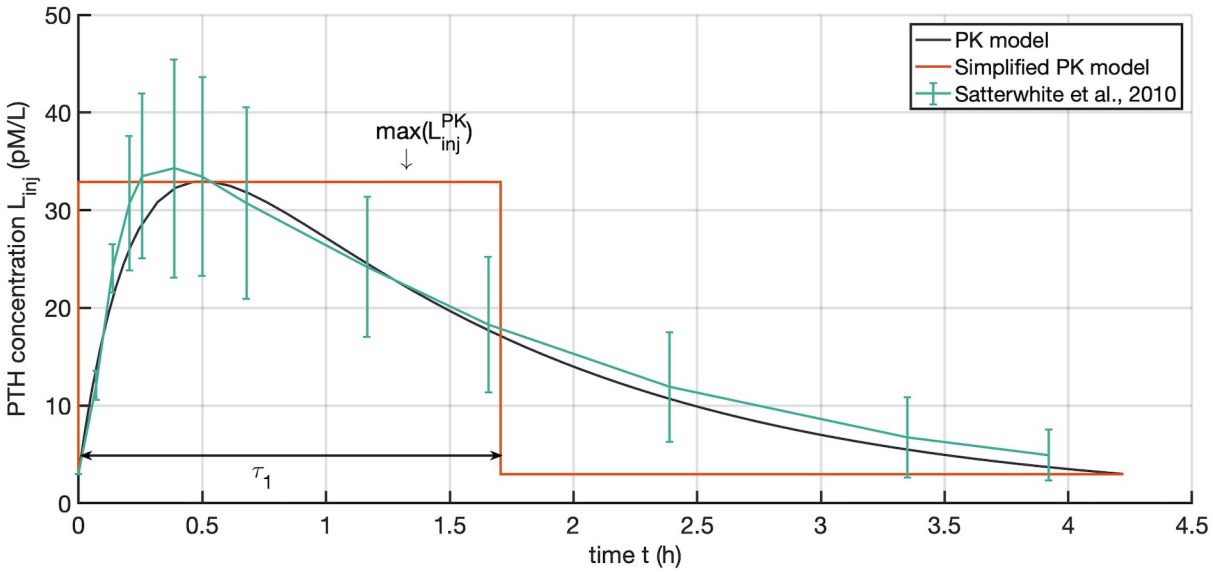

Fig 3. PTH plasma concentration obtained from the PTH PK model and the simplified square-wave stimulus characterised by the maximum PTH concentration $\max(L_{inj}^{PK})$ and the on-phase τ_1.

https://doi.org/10.1371/journal.pone.0283544.g003

drug concentration are equal between these two models ($A_{inj}^{PK} = A_{inj}$), we can calculate the on-phase of the square-wave signal as

$$\tau_1 = \frac{A_{inj}^{PK}}{\max(L_{inj}^{PK}) - \gamma_0}, \tag{13}$$

where γ_0 is the PTH concentration resulting from the tonic secretion, see Eq (10). The PTH drug concentration L_{inj} can be then approximated as

$$L_{inj}(D, T, \gamma_0, t) = \begin{cases} \gamma_1 & \text{if} \quad (n-1)T \le t \le (n-1)T + \tau_1 \\ \gamma_0 & \text{if} \quad (n-1)T + \tau_1 \le t \le (n-1)T + \tau_1 + \tau_0 \end{cases} \tag{14}$$

To compute the resulting *cellular responsiveness*, two models are investigated:

- model 1: we assume that the resulting PTH ligand concentration in Eq (1) is $L = L_{gl} + L_{inj}$, solve Eq (1) numerically and obtain the scaled activity from Eq (6) (blue curve in Fig 4(a)). Subsequently, the *cellular responsivenesses* α_R^{gl} and α_R^{inj} are computed separately by integrating over different parts of the scaled activity and scaling them with T_{gl} and T_{inj} for α_R^{gl} and α_R^{inj} in Eq (8), respectively. The resulting *cellular responsiveness* is computed as $\alpha_R = \alpha_R^{gl}(L) + \alpha_R^{inj}(L)$.
- model 2: Eq (1) is solved separately for both, L_{gl} and L_{inj}. Then, the *cellular responsiveness* is computed as $\alpha_R = \alpha_R^{gl}(L_{gl}) + \alpha_R^{inj}(L_{inj})$, see Fig 4b.

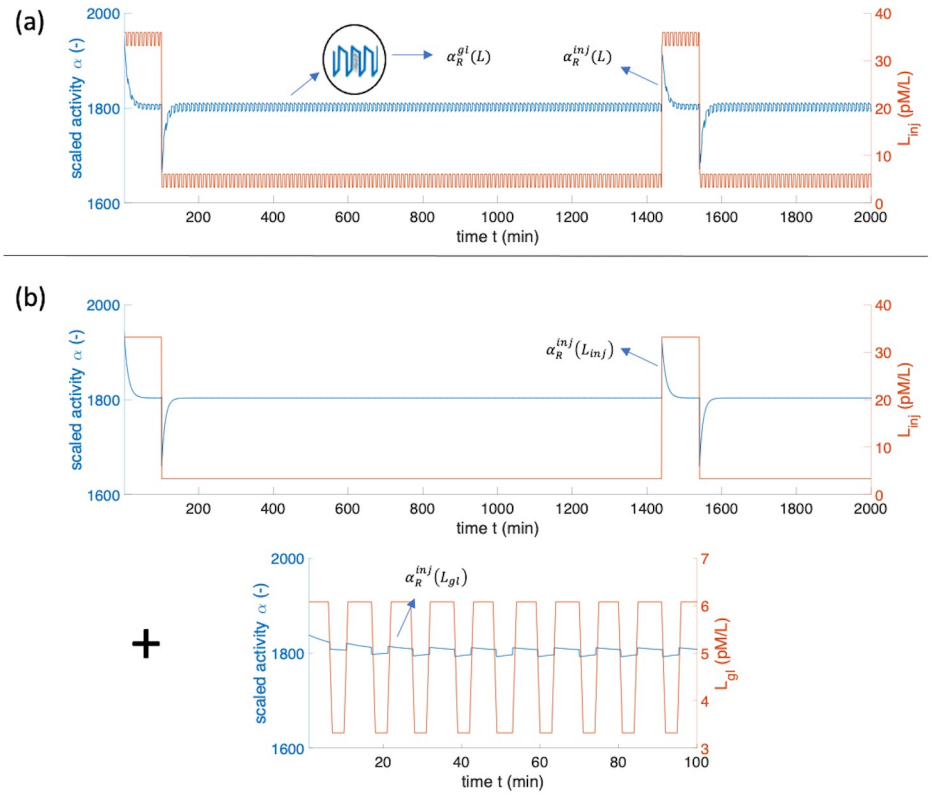

Fig 4. Computational simulation results of two models used to compute scaled activity α and *cellular responsiveness* α_R for the case of combined PTH glandular secretion and external sc daily PTH injection ($D = 20\mu g$). (a) refers to model 1 whereas (b) refers to model 2.

https://doi.org/10.1371/journal.pone.0283544.g004

Table 2. Computed *cellular responsiveness* for different PTH doses using model 1 and model 2.

daily drug dose D	healthy	idiopathic osteoporosis	hyperparathyroidism
0μg	0.939/0.939 (0)	0.497/0.497 (0)	2.105/2.105 (0)
10μg	1.358/1.398 (0.459)	0.957/0.957 (0.459)	2.376/2.443 (0.338)
20μg	1.778/1.818 (0.879)	1.375/1.376 (0.879)	2.694/2.835 (0.730)
30μg	2.143/2.183 (1.244)	1.759/1.741 (1.244)	3.042/3.179 (1.074)

Computed *cellular responsiveness* for different PTH doses administered via sc daily injections (model 1/model 2) superposed to baseline glandular secretion patterns. The results are given in form model 1 /model 2 (α_R^{inj}). For example, considering a healthy person and a PTH dose of 20μg, α_R computed from model 2 is obtained as a sum 0.939 + 0.879 = 1.818.

https://doi.org/10.1371/journal.pone.0283544.t002

Table 2 indicates that both models produce nearly the same *cellular responsiveness* α_R results for different doses and illnesses. Therefore, in the following computation, the computationally less expensive model 2 is utilised.

3 Optimal pulsatile regimes to reach maximal or targeted *cellular responsiveness*

We note that in the original work [16], a non-constrained optimisation for a square-wave signal with constant γ_0 and γ_1 was utilised. This is based on an analytical formula for an optimal τ_1 and T. However, as the numerical solution is available, different dosing patterns, i.e. combination of glandular and drug contribution (see Section 3.2) and different optimisation questions in addition to the maximisation of the *cellular responsiveness* can be answered. After transformation of the constrained optimisation problems to equivalent unconstrained ones, all optimisation problems are solved with the function *fminsearch* in MATLAB. In the following, we describe the formulation of different optimisation problems.

3.1 Baseline PTH secretion

As described earlier, the tonic secretion makes up approximately 70% and the pulsatile secretion the remaining 30%. Based on the data in [17, 18], the integrated concentration remain in the same range and hence we assume that the AUC in the (L, t)-plot can be rewritten as $A = A_{tonic} + A_{puls}$. To fix the mean plasma concentration at the reference value obtained from experimental data, we enforce that $A = A^{ref}$. In order to predict the optimal pulsatile pattern to reach the maximum *cellular responsiveness* α_R^{max}, we consider the following constrained optimisation problem

$$\max_{(\tau_1,T,\gamma_0,\gamma_1)} \alpha_R(L_{gl}(\tau_1, T, \gamma_0, \gamma_1, t)) \text{ with the constraints } \begin{cases} A(s, L_{gl}) = A^{ref}(s, L_{gl}) \\ A_{puls} = rA \end{cases} \tag{15}$$

where r is the ratio of pulsatile integrated concentration to total integrated concentration (see S1 Table), $A(s) = \int_0^s L_{gl}(\tau_1, T, \gamma_0, \gamma_1, t)\mathrm{d}t$ is the AUC in a (L_{gl}, t)-plot during an arbitrary time interval $[0, s]$ and the superscript *ref* refers to the quantities based on the experimental data for a healthy person [17, 18]. With the assumed square-wave stimulus in Eq (10) follows $A(s) = \gamma_0 s + \frac{(\gamma_1-\gamma_0)\tau_1 s}{T}$. The constraints in Eq (15) yield then

$$\gamma_0 = \gamma_0^{ref} \tag{16}$$

$$T = s\tau_1(\gamma_1 - \gamma_0)/rA^{ref} \tag{17}$$

Therefore, the constrained optimisation problem in Eq (15) can be reduced to a non-constrained optimisation problem

$$\boxed{\max_{(\gamma_1,\tau_1)} \alpha_R(L_{gl}(\tau_1, T, \gamma_0, \gamma_1, t))} \tag{18}$$

with γ_0 and T according to Eqs (16) and (17).

Another important question that can be addressed using the proposed optimisation method is "Can a healthy *cellular responsiveness* α_R^{ref} be reached by manipulating the glandular secretion pattern?". Note that the case of external PTH injection is considered below. Here, we explore the possibility of modulating a pathological glandular secretion pattern such that one would obtain α_R close to the healthy case. To answer the question if it is possible to reach the *cellular responsiveness* of the healthy person solely by changing the pulsatile pattern and keeping the area A constant, the following minimisation problem is to be solved

$$\boxed{\min_{(\gamma_1,\tau_1)}(\alpha_R(L_{gl}(\tau_1, T, \gamma_0, \gamma_1, t) - \alpha_R^{ref}))^2} \tag{19}$$

3.2 PTH injection

The previous concept can be applied to the investigation of the optimal dosing regimes for sc PTH injection and furthermore extended to other drugs. Here, we remark that τ_1 and γ_1 are not independent as they are given by the injected dose of the ligand and the experimentally measured pharmacokinetics. This is approximated by a function $f_{PK}(\gamma_0, D)$ determining the corresponding values, i.e. $(\gamma_1, \tau_1) = f_{PK}(\gamma_0, D)$. For different PTH daily doses ($D \in \{10\mu g, 20\mu g, 30\mu g\}$), *cellular responsiveness* is computed exemplarily for healthy person and patients with idiopathic osteoporosis and hyperparathyroidism.

3.2.1 Maximising the *cellular responsiveness*. Let A_{inj} be the AUC in the (L, t)-plot resulting from the sc injection of PTH (see Fig 4) and A_{inj}^{ref} the reference area corresponding the clinically used doses of 20μg once daily. The optimisation problem becomes

$$\boxed{\max_{(D,T)} \alpha_R^{inj}(D, T, \gamma_0) \text{ with the constraint } A_{inj}(D, T, \gamma_0) = A_{inj}^{ref}.} \tag{20}$$

which again is equivalent to a non-constrained optimisation

$$\boxed{\max_{D} \alpha_R^{inj}(D, T, \gamma_0)} \tag{21}$$

with $T = \tau_1(\gamma_1 - \gamma_0)/A_{inj}^{ref}$ and $(\gamma_1, \tau_1) = f_{PK}(\gamma_0, D)$ are given by the PK model [37].

3.2.2 Targeting healthy *cellular responsiveness* using external PTH injections. Suppose that α_R^{ill} denotes an altered *cellular responsiveness* compared to a healthy reference value α_R^{ref}, e.g. for patients with osteoporosis. Note that this could be higher or lower than α_R^{ref}. We are aiming to find a dose D such that the *cellular responsiveness* of the healthy person is reached, i.e. we solve the following optimisation problem

$$\boxed{\min_{D}(\alpha_R^{inj}(D, T, \gamma_0) - (\alpha_R^{ref} - \alpha_R^{ill}))^2.} \tag{22}$$

This gives the optimal dose to normalise the PTH *cellular responsiveness* by keeping the dosing period unchanged ($T = 24$ h).

4 Results of numerical simulations

4.1 Basal secretion

Table 3, first row, shows computed α_R using the mean experimental data [8, 17, 18] for healthy people and patients with different types of osteoporosis, hyperparathyroidism as well as under hyper- and hypocalcemia conditions. We note that if the tonic secretion is reduced in a healthy person, then the *cellular responsiveness* is slightly higher than the reference value. The corresponding scaled activity α computed according to Eq (6) is displayed in Fig 5, exemplarily for three cases with reference, reduced and increased α values—healthy, idiopathic osteoporosis and hyperparathyroidism, respectively.

In Table 3, solutions of the optimisation problems given in Eqs (18) and (19) are summarised. Superscript *max* denotes the values yielding the maximal *cellular responsiveness* by conserving the area A. Superscript * refers to the optimal values needed to reach the *cellular responsivenesss* of a healthy person. We note that this is possible only if $\alpha_R^{max} \geq \alpha_R^{ref}$.

Fig 6 shows surface plots where α_R for a healthy person is a function of two variables of the triplet (τ_1, T, γ_1). The third component is computed from Eq (17). The maximal *cellular responsiveness* is in each plot labelled with a red star. Its value $\alpha_R^{max} = 3.35$ is for all three cases identical because the same constrained optimisation problem given in Eq (15) is solved.

4.2 PTH external injection

In the following, simulation results for various PTH dosing patterns are presented with the aim of identifying optimal dosing regimes leading to maximum cellular responsiveness. Further, an optimal PTH dose of 9.61μg daily has been computed in order to reach the target *cellular responsiveness* of a patient with osteoporosis, see Table 4. The intersection of the red and black dashed lines in Fig 7 visually confirms that the optimal dose is close to 10μg. The latter figure also indicated that the *cellular responsiveness* increases nearly linearly as the daily dose increases.

Table 3. *Cellular responsiveness* for gland secretion.

parameter	healthy [17], r	OP	PMO [38, 39]	GIO	HP	hypocal 1	hypocal 2	hypercal
α_R	0.939/0.957	0.497	0.939/0.856	1.607	2.105	4.645	1.814	0.174
α_R^{max}	3.345/3.384	0.649	3.345/2.757	5.689	9.983	27.653	6.798	0.466
τ_1^{max} (min)	12.92/12.89	11.77	12.92/12.64	13.49	14.78	15.67	14.24	11.33
T^{max} (min)	54.94/54.31	65.94	55.94/55.57	51.23	55.04	50.01	55.12	65.78
γ_1^{max} (pm/L)	10.41/9.68	4.98	10.41/8.52	12.67	38.73	78.18	25.63	1.99
τ_1^* (min)	6.40/6.54	-	6.40/6.46	6.33	7.80	-	6.42	-
T^* (min)	10.60/10.69	-	10.60/11.50	8.94	9.80	-	8.84	-
γ_1^* (pm/L)	6.08/5.38	-	6.08/5.02	5.71	22.21	-	15.45	-

Cellular responsiveness α_R for gland secretion computed according to Eq (8), α_R and the corresponding τ_1, T, γ_1 are denoted with the superscripts *max* and * as solutions of the optimisation problems in Eqs (18) and (19), respectively. Coding: healthy = healthy person [17], r = healthy with reduced (by 20%) tonic secretion, OP = idiopathic osteoporosis [17], PMO = postmenopausal osteoporosis based on [38, 39], GIO = glucorticoid-induced osteoporosis [40], HP = hyperparathyroidism [18], hypocal 1 = hypocalcemia initial state [32], hypocal 2 = hypocalcemia steady state [32], hypercal = hypercalcemia steady state [32]. - optimisation problem (19) has no solution within the tolerance. Simulation parameters are given in Table 1 and S2 Table.

https://doi.org/10.1371/journal.pone.0283544.t003

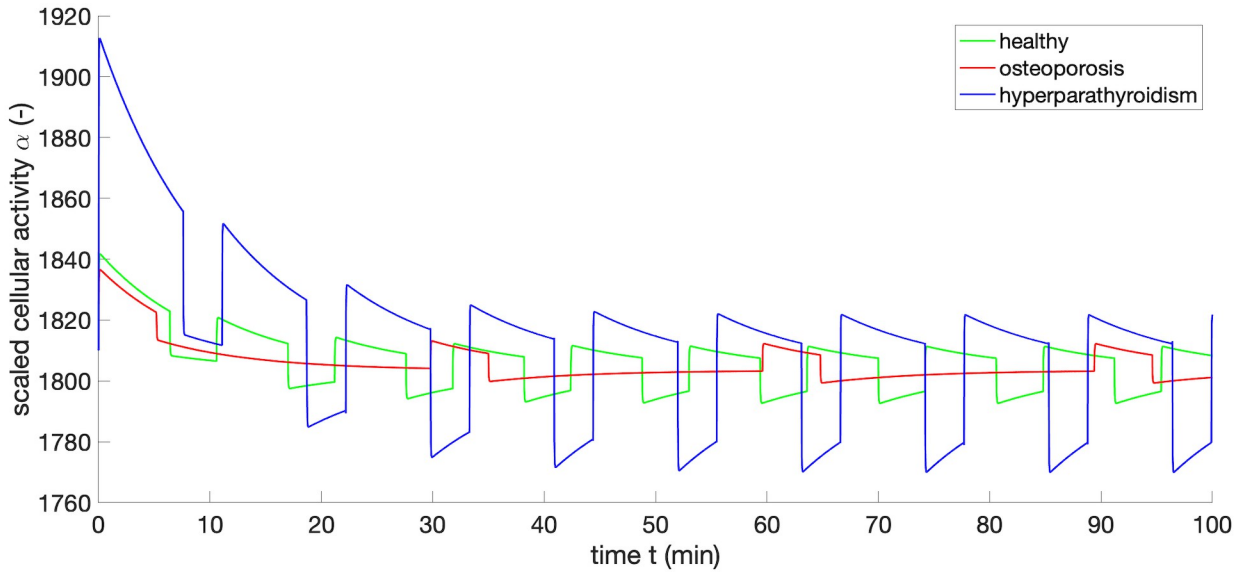

Fig 5. Scaled activity α for healthy person, patient with idiopathic osteoporosis and hyperparathyroidism. Simulation parameters are given in Table 1 and S2 Table.

https://doi.org/10.1371/journal.pone.0283544.g005

5 Discussion

In this paper, we utilised a two-state receptor model to investigate bone cellular responses due to PTH glandular secretion patterns together with external administration of PTH. We considered five different types of glandular secretion patterns corresponding to healthy subjects and patients with osteoporosis, hyperparathyroidism, hypercalcemia and hypocalcemia. Our model a priori prescribes a particular glandular PTH secretion pattern reported in the literature and then calculates the corresponding cellular activity. We note that the PTH glandular secretion plays a pivotal role in calcium and phosphorus homeostasis and, consequently,

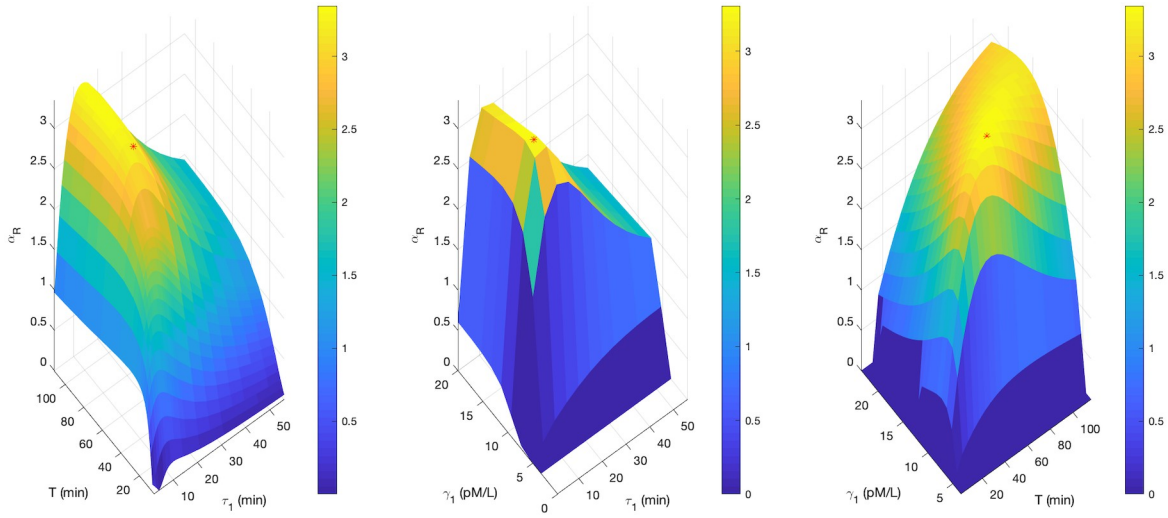

Fig 6. *Cellular responsiveness* for a healthy person as function of T and τ_1; γ_1 and τ_1; γ_1 and T. The third quantity of the triplet (γ_1, τ_1, T) results from the optimisation constraint given in Eq (15). Simulation parameters are given in Table 1 and S2 Table.

https://doi.org/10.1371/journal.pone.0283544.g006

Table 4. Maximum *cellular responsiveness* for PTH doses administered via sc daily injections.

parameter	10μg	20μg	30μg	optimised dose according to Eq (22)	
α_R^{max}	1.455	2.183	2.817	$\alpha_R^{ref}/\alpha_R^{ill}$	0.939/0.497
D^{max} (μg)	1.606	2.866	4.049	D^*	9.61
τ_1^{max} (min)	43.30	58.76	67.67	τ_1^*	87.90
T^{max} (min)	79.18	98.56	107.60	T	1440
γ_1^{max} (pM/L)	6.63	8.51	10.32	γ_1^*	17.16

Maximum *cellular responsiveness* for PTH doses administered via sc daily injections given to a patient with osteoporosis. Model 2 is used for optimisation. Superscript *max* denotes values leading to maximum *cellular responsiveness* α_R^{max} by keeping the daily drug dose, i.e. the area A_{inj} unchanged. Superscript * denotes the optimal values to reach the reference *cellular responsiveness* α_R^{ref}.

https://doi.org/10.1371/journal.pone.0283544.t004

factors that affect the different organs involved in controlling mineral balance can also influence the glandular secretion patterns. Major factors that can affect PTH glandular secretion are dietary conditions (i.e., calcium and phosphorus intake), lifestyle (i.e., physical activity), and genetics (i.e., vitamin D system). However, it is beyond the scope of the current study to investigate the effects of these factors on glandular PTH secretion patterns.

Using an efficient numerical approach to solve the ODEs allowed us to formulate a variety of optimisation problems which aimed at restoring the perturbed bone cellular response due to different disease back to the healthy baseline state. We note that the computation of the *cellular responsiveness* based on a two-state receptor model is for the first time computed numerically. The numerical approach is much more flexible in the sense that there are no special case restrictions on the parameters in the model and one can easily consider different scenarios by formulating constrained optimisation problems with various objective functions and constraints. The MATLAB codes are provided on request.

Below, we discuss first how the different bone cell response values can be interpreted in a bone remodelling context. Then, we discuss the manipulation of glandular secretion patterns

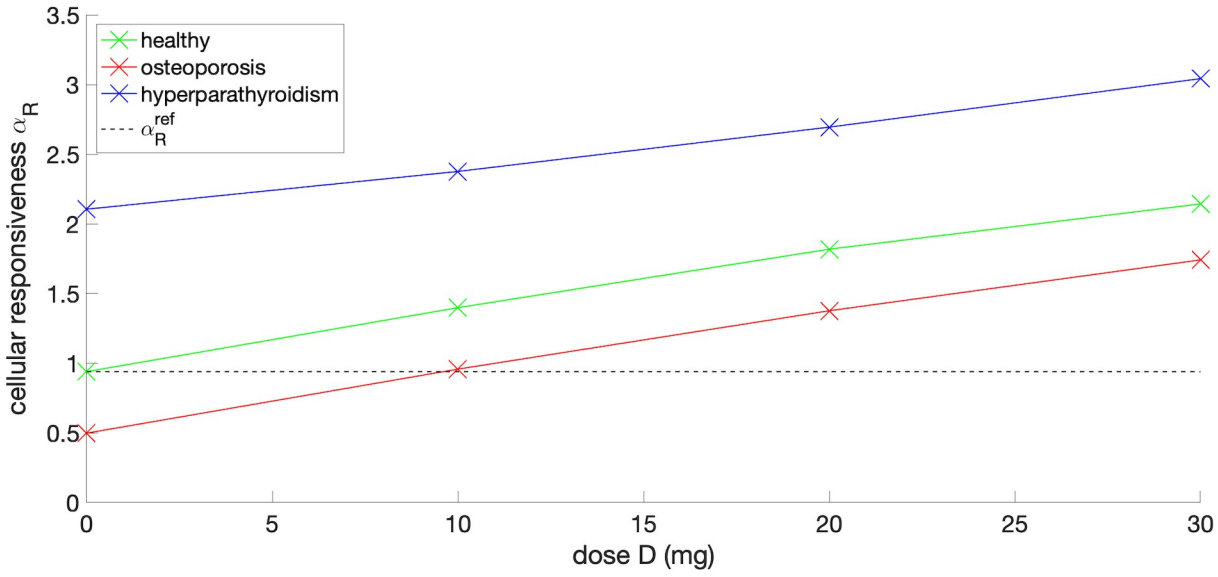

Fig 7. *Cellular responsiveness* computed with model 2 for healthy person, patients with idiopathic osteoporosis and hyperparathyroidism after different doses of PTH sc injection are applied once daily.

https://doi.org/10.1371/journal.pone.0283544.g007

and the superposition of an external PTH injections. Finally, we will also discuss the limitations of the current study.

5.1 Comparison of healthy versus disease states

While the bone cellular response parameter (α_R) of the current two-state receptor model is not linked to any (downstream) catabolic or anabolic bone cell responses, it is instructive to view this parameter's action on the bone remodelling process. In the bone remodelling models of Lemaire et al. and Pivonka et al. [41–43], a single monovalent binding reaction function was used to simulate the catabolic action of PTH on bone remodelling. This was achieved by introducing a PTH activator function which was a sigmoidal function of the PTH serum concentration mapped on the interval 0 and 1. Using this function, the catabolic ligand (RANKL) expressed on osteoblastic cells was monotonously increased for pathological cases of increased PTH serum concentration. We note that serum PTH concentration was assumed constant in these models and based on the rather simplistic receptor ligand binding model, it was emphasised that these models are not able to capture pulsatile effects of PTH such as the anabolic response due to external intermittent PTH injections. Hence, a reduction in serum PTH concentration gave rise to reduced bone remodelling with modest to no anabolic bone gains.

In the following, we interpret the decrease or increase of α_R with respect to catabolic actions of bone cells on the remodelling process. Hence, an increased value of the bone cellular response parameter (compared to the healthy baseline value) indicates a catabolic response, while a decreased value of α_R indicates a moderate anabolic bone response. With this in mind, the simulation results for hyperparathyroidism and hypocalcemia indicate that for the given pattern of glandular PTH secretion, a catabolic bone response is obtained. Hence, for these pathological conditions, net increase in bone resorption will occur. Primary hyperparathyroidism is due to a benign overgrowth of parathyroid tissue either as single gland (80% of cases) or as a multiple gland disorder. For symptomatic cases, it is associated with bone loss. The latter can be treated by using antiresorptive drugs, but more often hyperparathyroidism can be cured by removing the parathyroid gland(s) [6].

For the hypocalcemia simulations representing the hypocalcemic clamp tests reported in [32], we found that the PTH glandular secretion pattern in the transitional period of hypocalcemia (i.e., hypocalcemia 1) gave rise to a very high α_R value indicating high bone resorption, while the α_R value for the steady state period was significantly lower indicating lower bone resorption. Based on the tight regulation of calcium homeostasis, these results are meaningful, i.e. the immediate reduction of calcium due to the clamp test is rapidly compensated for by high bone resorption followed by a more modest bone resorption period.

For the hypercalcemia simulations representing the hypercalcemic clamp test reported in [32], we found that the PTH glandular secretion pattern led to a lower value of α_R and consequently reducing bone remodelling. During bone remodelling calcium is released from the bone matrix and, consequently, reducing bone remodelling avoids release of calcium into the plasma [44].

For the case of the osteoporosis simulations, lower, approximately similar and higher α_R values compared to healthy baseline were obtained for the idiopathic osteoporosis (OP), postmenopausal osteoporosis (PMO) and glucocorticoid-induced osteoporosis (GIO) case, respectively. Below we interpret these results in more detail. The results for the idiopathic OP seem to be not physiologically meaningful given that osteoporosis is associated with bone loss (i.e., catabolic bone response) [45]. However, there are quite a number of things to consider for interpretation of this result. The OP data [17] are based on only three male patients with idiopathic OP (mean age, 37 yr; range, 31–42 yr). This is an extremely low sample number. Also,

research into establishing a link between PTH patterns and other types of osteoporosis indicate that PTH modulation may be only a secondary effect, but that other catabolic bone regulators (such as RANKL) could directly be affected by the disease. Below, we discuss some of these findings.

For cases of PMO, our simulation results indicate that α_R is equal or slightly reduced compared to the reference value. These results are based on qualitative data provided in [8] for describing the PTH glandular secretion pattern in PMO. However, the data on this pattern are not conclusive as discussed next. Samuels et al. [38] compared PTH glandular secretion patterns from healthy young subjects with postmenopausal women of various oestrogen levels and bone mineral density (BMD). They found there were no differences in the amplitude or frequency of pulsatile PTH secretory parameters between the pathological cases and the healthy group. They concluded that different types of PMO do not alter PTH secretory patterns and temporal organisation. Based on these findings, the authors suggested that abnormalities in orderly pulsatile PTH secretion are unlikely to play a major role in driving PMO related osteoporosis. We note that oestrogen deficiency, i.e. a hallmark of PMO, has been directly linked with increased RANKL production.

For the case of GIO, which is the largest cause of secondary osteoporosis, some studies have not found an association between GIO and increased PTH concentration. On the other hand, other studies have shown that patients with GIO did exhibit elevated PTH serum concentrations [46]. However, as pointed out in [8], the PTH serum levels have little meaning in identifying a role of PTH in driving GIO, but it is the glandular pulsatile secretory pattern of PTH that might provide a link. However, only a few studies have investigated this pattern in a very small population of men. Bonadonna et al. [40] evaluated spontaneous PTH pulsatile secretion in patients chronically treated with pharmacological amounts of glucocorticoids. Their findings indicate that in the glucocorticoid-treated group, the PTH tonic secretory rate was reduced, while there was an increase in the fractional pulsatile PTH secretion in glucocorticoid-treated vs normal subjects. Mean overall PTH concentration, as well as mean integrated area, was similar among normal and glucocorticoid-treated subjects. Therefore, it can be concluded that chronic glucocorticoid treatment induces a redistribution of spontaneous PTH secretory dynamics by reducing the amount released in tonic fashion and increasing the amount released as pulses. In this study, GIO is simulated by scaling the parameters τ_1, T, γ_0 and γ_1 according to the data provided in [40], see S2 Table. In particular, the tonic secretion is nearly halved while the pulsatile pattern remains similar as the reference values. Our simulation produces α_R value significantly larger than in the healthy case. This indicates bone resorption which is in agreement with the obtained findings.

5.2 Optimisation of glandular dosing patterns to restore healthy cell response

Our simulation results for some of the PTH glandular disease states indicate that it may be possible to pharmacologically manipulate the PTH secretion pattern such as to restore similar values for *cellular responsiveness* as for healthy subjects. This would indicate a similar bone remodelling behaviour. We note that this could only be achieved for pathological cases that led to $\alpha_R^{max}/\alpha_R^{min}$ values higher/lower than the healthy baseline value, i.e. PMO, hyperparathyroidism, hypocalemia clamp test, and GIO. These cases, except PMO, could be restored towards the healthy α_R^{ref} by manipulating the pulsatile profile to a more continuous pattern which desensitises the active receptors and ligand complexes and leads to lower values of α_R. For PMO, solely the manipulation of the pulsatile pattern leads to an elevation of α_R up to the reference value. On the other hand, PTH glandular diseases that led to maximum bone *cellular*

responsiveness below the healthy baseline value such as the idiopathic osteoporosis case reported by Harms et al. [17], can't be restored to baseline via glandular manipulation. For such cases, external PTH injections are a viable solution which is further discussed below. Moreover, in the case of the initial hypercalcemia, the minimum *cellular responsiveness* α_R^{min} is higher than α_R^{ref} and therefore a lowering to the targeted level is not possible, too.

5.3 Effects of external PTH injections

To simulate the effect of external sc once daily PTH administration, as it is currently clinically available, one had to superpose the external PTH injection with the glandular PTH secretion. We explored two modelling approaches: In model 1, we assume that the resulting PTH ligand concentration in Eq (1) becomes $L = L_{gl} + L_{inj}$. Subsequently, Eq (1) is solved numerically. In model 2, Eq (1) is solved separately for both, L_{gl} and L_{inj}. Then, the α_R is given as a sum of the *cellular responsiveness* of the gland and a sc injection. Comparison of the simulation results for these two models indicated that the final values for α_R are very similar. Given that the computational efficiency of model 2 was significantly higher than model 1, all optimisations were performed for model 2. A general observation is, that superposing external PTH injections onto a baseline glandular secretion gave rise to increased values of α_R. The increase of the *cellular responsiveness* scaled nearly linearly with respect to the external PTH dose. Hence, for the case of osteoporosis, optimum external PTH dose of $D = 10\mu$g daily injections, that would give a *cellular responsiveness* close to the healthy state.

5.4 Limitations of the current study

The current study has a number of limitations. The receptor ligand PTH-PTH1R binding constants are taken from the open literature. We note that we deliberately did not use the constants that were proposed in [15] for several reasons. Firstly, the constants are not experimentally determined and do not fulfil the condition of the detailed balance as proposed [16]. Secondly, using the constants suggested in [15] gives several orders of magnitude difference between the active complexes and inactive complexes, which seems physiologically not realistic.

Another limitation of our study is that we discussed mainly the action of PTH on RANKL expression on cells of the osteoblastic lineage with no discussions of potential feedback mechanisms in the organs responsible for mineral metabolism. One such factor is fibroblast growth factor 23 (FGF-23) which is most highly expressed in bone, predominantly in osteocytes [47, 48]. In healthy subjects FGF-23 is expressed at low levels in osteocytes, but is significantly increased in osteocytes in patients with hypophosphatemic rickets [49] and in patients with chronic kidney disease [50]. It has been suggested that circulating FGF-23 directly acts on parathyroid glands to modify PTH dosing pattern [51].

We acknowledge that the current study exclusively focused on the PTH-PTH1R system that is most relevant for regulation of bone metabolism. We note that PTH also binds to its second receptor PTH2R together with its Ligand Tuberoinfundibular Peptide of 39 Residues (TIP39) to particularly regulate skin function via differentiation of keratocytes [52].

6 Conclusions

We developed a novel two-state PTH-PTH1R receptor binding model to analyse the effects of PTH glandular secretion patterns on bone *cellular responsiveness*. In particular, we explored differences between healthy and pathological glandular secretion patterns and their effect on bone cellular responsiveness. We explored the potential of (pharmacological) manipulation of

pathological glandular secretion patterns back to its normal baseline bone cellular responsiveness. Also, we investigated the effect of (external) once daily PTH injections on bone cellular responsiveness. For this purpose, we formulated a variety of constrained optimisation problems with and without keeping the area under the curve constant. Based on our numerical simulations, we found the following:

- Bone *cellular responsiveness* in healthy subjects is sensitive to the tonic baseline stimulus and is significantly below the maximum responsiveness;
- Bone *cellular responsiveness* greatly varies between healthy and pathological glandular secretions patterns;
- Catabolic bone diseases, as defined by $\alpha_R^{ill} > \alpha_R^{ref}$, (with exception of very high hypocalcemia) could be restored to normal by manipulating the pulsatile component of glandular secretion of the pathological gland;
- Bone diseases characterised by $\max(\alpha_R^{ill}) < \alpha_R^{ref}$ with a maximum *cellular responsiveness* value below healthy baseline can't be restored to baseline.
- External once daily PTH injections can restore the above cases back to normal.
- Superposition of glandular PTH secretion and external PTH injections can be effectively achieved by additive superposition;
- Based on the numerical formulation of the two-state receptor model, constrained optimisation problems can be efficiently formulated and solved;

In conclusion, the current two-state receptor model seems to capture major aspect of PTH glandular secretion and associated skeletal pathologies. In the future, this type of model could be used for analysing pharmacological drug effects on glandular secretion.

Supporting information

S1 Table. Experimental data. Experimental data for PTH, based on the cited literature. The values are given as mean ± sd or median (minimum—maximum).
(PDF)

S2 Table. Simulation parameters. Simulation parameters for cases: healthy person [17]/ healthy with reduced (by 20%) tonic secretion, idiopathic osteoporosis (OP), postmenopausal osteoporosis (PMO), glucocorticoid induced osteoporosis (GIO), initial hypocalcemia (hypocal 1), steady state hypocalcemia (hypocal 2) and hypercalcemia (hypercal) and glucocorticoid induced osteoporosis (GIO). The parameters for healthy person, OP and HP are based on the experimental provided in [17] which are shown in S1 Table. The remaining parameters are obtained via scaling the experimental data for healthy people [17] with relative changes presented in [38–40, 53] for PMO, GIO and different calcium levels, respectively.
(PDF)

Author Contributions

Conceptualization: Denisa Martonová, Sigrid Leyendecker, Peter Pivonka.

Funding acquisition: Sigrid Leyendecker, Peter Pivonka.

Investigation: Peter Pivonka.

Methodology: Denisa Martonová, Maxence Lavaill, Sigrid Leyendecker, Peter Pivonka.

Resources: Sigrid Leyendecker, Peter Pivonka.

Software: Denisa Martonová, Maxence Lavaill.

Supervision: Sigrid Leyendecker, Peter Pivonka.

Visualization: Denisa Martonová.

Writing – original draft: Denisa Martonová, Peter Pivonka.

Writing – review & editing: Maxence Lavaill, Mark R. Forwood, Alexander Robling, David M. L. Cooper, Sigrid Leyendecker, Peter Pivonka.

References

1. Hernández-Castellano LE, Hernandez LL, Bruckmaier RM. Review: Endocrine Pathways to Regulate Calcium Homeostasis around Parturition and the Prevention of Hypocalcemia in Periparturient Dairy Cows. Animal. 2020; 14(2):330–338. https://doi.org/10.1017/S1751731119001605 PMID: 31337460
2. Wendelaar Bonga SE, Pang PK. Control of Calcium Regulating Hormones in the Vertebrates: Parathyroid Hormone, Calcitonin, Prolactin, and Stanniocalcin. International Review of Cytology. 1991; 128:139–213. https://doi.org/10.1016/S0074-7696(08)60499-4 PMID: 1917377
3. Brown EM. Extracellular Ca2+ Sensing, Regulation of Parathyroid Cell Function, and Role of Ca2+ and Other Ions as Extracellular (First) Messengers. Physiological Reviews. 1991. https://doi.org/10.1152/physrev.1991.71.2.371 PMID: 2006218
4. Mundy GR, Martin TJ. Physiology and Pharmacology of Bone. vol. 107 of Handbook of Experimental Pharmacology. Berlin, Heidelberg: Springer Berlin Heidelberg; 1993.
5. Cheloha RW, Gellman SH, Vilardaga JP, Gardella TJ. PTH receptor-1 signalling—mechanistic insights and therapeutic prospects. Nature Reviews Endocrinology. 2015; 11(12):712–724. https://doi.org/10.1038/nrendo.2015.139 PMID: 26303600
6. Bilezikian JP, Bandeira L, Khan A, Cusano NE. Hyperparathyroidism. Lancet (London, England). 2018; 391(10116):168–178. https://doi.org/10.1016/S0140-6736(17)31430-7 PMID: 28923463
7. Dean T, Vilardaga JP, Potts J J T, Gardella TJ. Altered Selectivity of Parathyroid Hormone (PTH) and PTH-Related Protein (PTHrP) for Distinct Conformations of the PTH/PTHrP Receptor. Molecular Endocrinology. 2008; 22(1):156–166. https://doi.org/10.1210/me.2007-0274 PMID: 17872377
8. Chiavistelli S, Giustina A, Mazziotti G. Parathyroid Hormone Pulsatility: Physiological and Clinical Aspects. Bone Research. 2015; 3(1):1–5. https://doi.org/10.1038/boneres.2014.49 PMID: 26273533
9. Schmitt CP, Hömme M, Schaefer F. Structural Organization and Biological Relevance of Oscillatory Parathyroid Hormone Secretion. Pediatric Nephrology (Berlin, Germany). 2005; 20(3):346–351. https://doi.org/10.1007/s00467-004-1767-7 PMID: 15700141
10. Merriam GR, Wachter KW. Algorithms for the Study of Episodic Hormone Secretion. The American Journal of Physiology. 1982; 243(4):E310–318. PMID: 6889816
11. Veldhuis JD, Johnson ML. Cluster Analysis: A Simple, Versatile, and Robust Algorithm for Endocrine Pulse Detection. American Journal of Physiology-Endocrinology and Metabolism. 1986; 250(4):E486–E493. https://doi.org/10.1152/ajpendo.1986.250.4.E486 PMID: 3008572
12. Santen RJ, Bardin CW. Episodic Luteinizing Hormone Secretion in Man. Pulse Analysis, Clinical Interpretation, Physiologic Mechanisms. The Journal of Clinical Investigation. 1973; 52(10):2617–2628. https://doi.org/10.1172/JCI107454 PMID: 4729055
13. Tay D, Cremers S, Bilezikian JP. Optimal dosing and delivery of parathyroid hormone and its analogues for osteoporosis and hypoparathyroidism—translating the pharmacology. British Journal of Clinical Pharmacology. 2018; 84(2):252–267. https://doi.org/10.1111/bcp.13455 PMID: 29049872
14. Segel LA, Goldbeter A, Devreotes PN, Knox BE. A Mechanism for Exact Sensory Adaptation Based on Receptor Modification. Journal of Theoretical Biology. 1986; 120(2):151–179. https://doi.org/10.1016/S0022-5193(86)80171-0 PMID: 3784578
15. Potter LK, Greller LD, Cho CR, Nuttall ME, Stroup GB, Suva LJ, et al. Response to Continuous and Pulsatile PTH Dosing: A Mathematical Model for Parathyroid Hormone Receptor Kinetics. Bone. 2005; 37(2):159–169. https://doi.org/10.1016/j.bone.2005.04.011 PMID: 15921971

16. Li Y, Goldbeter A. Frequency Specificity in Intercellular Communication. Influence of Patterns of Periodic Signaling on Target Cell Responsiveness. Biophysical Journal. 1989; 55(1):125–145. https://doi.org/10.1016/S0006-3495(89)82785-7 PMID: 2930817

17. Harms HM, Kaptaina U, Külpmann WR, Brabant G, Hesch RD. Pulse Amplitude and Frequency Modulation of Parathyroid Hormone in Plasma*. The Journal of Clinical Endocrinology & Metabolism. 1989; 69(4):843–851. https://doi.org/10.1210/jcem-69-4-843 PMID: 2778038

18. Harms HM, Schlinke E, Neubauer O, Kayser C, Wüstermann PR, Horn R, et al. Pulse Amplitude and Frequency Modulation of Parathyroid Hormone in Primary Hyperparathyroidism. 1994; p. 5.

19. Silverberg SJ, Bone HG, Marriott TB, Locker FG, Thys-Jacobs S, Dziem G, et al. Short-Term Inhibition of Parathyroid Hormone Secretion by a Calcium-Receptor Agonist in Patients with Primary Hyperparathyroidism. The New England Journal of Medicine. 1997; 337(21):1506–1510. https://doi.org/10.1056/NEJM199711203372104 PMID: 9366582

20. Trivedi R, Mithal A, Chattopadhyay N. Recent Updates on the Calcium-Sensing Receptor as a Drug Target. Current Medicinal Chemistry. 2008; 15(2):178–186. https://doi.org/10.2174/092986708783330601 PMID: 18220773

21. Weiss JA, Makerc BN, Govindjee S. Finite Element Implementation of Incompressible, Transversely Isotropic Hyperelasticity. Comput Methods Appl Mech Engrg. 1996; 135(1-2):107–128. https://doi.org/10.1016/0045-7825(96)01035-3

22. Lauffenburger DA, Linderman J. Receptors: Models for Binding, Trafficking, and Signaling. Revised edition ed. New York, NY: Oxford University Press; 1996.

23. Structure and Function of 7-TM G-Protein Coupled Receptors. In: Foreman JC, Johansen T, Gibb AJ, editors. Textbook of Receptor Pharmacology. 3rd ed. CRC Press; 2010.

24. Waelbroeck I. Kinetics versus Equilibrium: The Importance of GTP in GPCR Activation. Trends in Pharmacological Sciences. 1999; 20(12):477–481. https://doi.org/10.1016/S0165-6147(99)01394-2 PMID: 10603489

25. Parfitt AM. Parathyroid Hormone and Periosteal Bone Expansion. Journal of Bone and Mineral Research. 2002; 17(10):1741–1743. https://doi.org/10.1359/jbmr.2002.17.10.1741 PMID: 12369776

26. Gardella TJ, Jüppner H. Molecular Properties of the PTH/PTHrP Receptor. Trends in endocrinology and metabolism: TEM. 2001; 12(5):210–217. https://doi.org/10.1016/S1043-2760(01)00409-X PMID: 11397646

27. Leff P. The two-state model of receptor activation. Trends in Pharmacological Sciences. 1995; 16 (3):89–97. https://doi.org/10.1016/S0165-6147(00)88989-0 PMID: 7540781

28. Trichilo S, Scheiner S, Forwood M, Cooper DML, Pivonka P. Computational Model of the Dual Action of PTH—Application to a Rat Model of Osteoporosis. Journal of Theoretical Biology. 2019; 473:67–79. https://doi.org/10.1016/j.jtbi.2019.04.020 PMID: 31009612

29. Yasuoka T, Kawashima M, Takahashi T, Iwata A, Oka N, Tanaka K. Changes in Parathyroid Hormone Receptor Binding Affinity during Egg Laying: Implications for Calcium Homeostasis in Chicken. Journal of Bone and Mineral Research. 2010; 11(12):1913–1920. https://doi.org/10.1002/jbmr.5650111212

30. Hoare SRJ, Usdin TB. Quantitative Cell Membrane-Based Radioligand Binding Assays for Parathyroid Hormone Receptors. Journal of Pharmacological and Toxicological Methods. 1999; 41(2-3):83–90. https://doi.org/10.1016/S1056-8719(99)00024-6 PMID: 10598679

31. Martiel JL, Goldbeter A. A Model Based on Receptor Desensitization for Cyclic AMP Signaling in Dictyostelium Cells. Biophysical Journal. 1987; 52(5):807–828. https://doi.org/10.1016/S0006-3495(87)83275-7 PMID: 19431710

32. Schmitt CP, Schaefer F, Bruch A, Veldhuis JD, Schmidt-Gayk H, Stein G, et al. Control of Pulsatile and Tonic Parathyroid Hormone Secretion by Ionized Calcium. The Journal of Clinical Endocrinology and Metabolism. 1996; 81(12):4236–4243. https://doi.org/10.1210/jcem.81.12.8954021 PMID: 8954021

33. Schaefer F. Pulsatile Parathyroid Hormone Secretion in Health and Disease. In: Chadwick DJ, Goode JA, editors. Novartis Foundation Symposia. Chichester, UK: John Wiley & Sons, Ltd; 2008. p. 225–243.

34. Samuels MH, Veldhuis J, Cawley C, Urban RJ, Luther M, Bauer R, et al. Pulsatile Secretion of Parathyroid Hormone in Normal Young Subjects: Assessment by Deconvolution Analysis. 1993; p. 5.

35. Veldhuis JD, Carlson ML, Johnson ML. The Pituitary Gland Secretes in Bursts: Appraising the Nature of Glandular Secretory Impulses by Simultaneous Multiple-Parameter Deconvolution of Plasma Hormone Concentrations. Proceedings of the National Academy of Sciences. 1987; 84(21):7686–7690. https://doi.org/10.1073/pnas.84.21.7686 PMID: 2823271

36. Fletcher PA, Clément F, Vidal A, Tabak J, Bertram R. Interpreting Frequency Responses to Dose-Conserved Pulsatile Input Signals in Simple Cell Signaling Motifs. PLoS ONE. 2014; 9(4):e95613. https://doi.org/10.1371/journal.pone.0095613 PMID: 24748217

37. Lavaill M, Trichilo S, Scheiner S, Forwood MR, Cooper DML, Pivonka P. Study of the Combined Effects of PTH Treatment and Mechanical Loading in Postmenopausal Osteoporosis Using a New Mechanistic PK-PD Model. Biomechanics and Modeling in Mechanobiology. 2020; 19(5):1765–1780. https://doi.org/10.1007/s10237-020-01307-6 PMID: 32100180

38. Samuels MH, Veldhuis JD, Kramer P, Urban RJ, Bauer R, Mundy GR. Episodic Secretion of Parathyroid Hormone in Postmenopausal Women: Assessment by Deconvolution Analysis and Approximate Entropy. Journal of Bone and Mineral Research. 1997; 12(4):616–623. https://doi.org/10.1359/jbmr.1997.12.4.616 PMID: 9101373

39. Harms HM, Neubauer O, Kayser C, Wüstermann PR, Horn R, Brosa U, et al. Pulse Amplitude and Frequency Modulation of Parathyroid Hormone in Early Postmenopausal Women before and on Hormone Replacement Therapy. The Journal of Clinical Endocrinology and Metabolism. 1994; 78(1):48–52. https://doi.org/10.1210/jcem.78.1.8288712 PMID: 8288712

40. Bonadonna S, Burattin A, Nuzzo M, Bugari G, Rosei EA, Valle D, et al. Chronic Glucocorticoid Treatment Alters Spontaneous Pulsatile Parathyroid Hormone Secretory Dynamics in Human Subjects. European Journal of Endocrinology. 2005; 152(2):199–205. https://doi.org/10.1530/eje.1.01841 PMID: 15745926

41. Lemaire V, Tobin FL, Greller LD, Cho CR, Suva LJ. Modeling the Interactions between Osteoblast and Osteoclast Activities in Bone Remodeling. Journal of Theoretical Biology. 2004; 229(3):293–309. https://doi.org/10.1016/j.jtbi.2004.03.023 PMID: 15234198

42. Pivonka P, Zimak J, Smith DW, Gardiner BS, Dunstan CR, Sims NA, et al. Model Structure and Control of Bone Remodeling: A Theoretical Study. Bone. 2008; 43(2):249–263. https://doi.org/10.1016/j.bone.2008.03.025 PMID: 18514606

43. Pivonka P, Zimak J, Smith DW, Gardiner BS, Dunstan CR, Sims NA, et al. Theoretical Investigation of the Role of the RANK-RANKL-OPG System in Bone Remodeling. Journal of Theoretical Biology. 2010; 262(2):306–316. https://doi.org/10.1016/j.jtbi.2009.09.021 PMID: 19782692

44. Rowe P, Koller A, Sharma S. Physiology, Bone Remodeling. In: StatPearls. Treasure Island (FL): StatPearls Publishing; 2022.

45. Sözen T, Özışık L, Başaran NÇ. An Overview and Management of Osteoporosis. European Journal of Rheumatology. 2017; 4(1):46–56. https://doi.org/10.5152/eurjrheum.2016.048 PMID: 28293453

46. Rubin MB, Bodner SR. A Three-Dimensional Nonlinear Model for Dissipative Response of Soft Tissue. International Journal of Solids and Structures. 2002; 39:5081–5099. https://doi.org/10.1016/S0020-7683(02)00237-8

47. Shimada T, Kakitani M, Yamazaki Y, Hasegawa H, Takeuchi Y, Fujita T, et al. Targeted Ablation of Fgf 23 Demonstrates an Essential Physiological Role of FGF 23 in Phosphate and Vitamin D Metabolism; 2004.

48. Bonewald LF, Wacker MJ. FGF23 Production by Osteocytes. Pediatric nephrology (Berlin, Germany). 2013; 28(4):563–568. https://doi.org/10.1007/s00467-012-2309-3 PMID: 22983423

49. Liu S, Rowe PSN, Vierthaler L, Zhou J, Quarles LD. Phosphorylated Acidic Serine-Aspartate-Rich MEPE-associated Motif Peptide from Matrix Extracellular Phosphoglycoprotein Inhibits Phosphate Regulating Gene with Homologies to Endopeptidases on the X-chromosome Enzyme Activity. The Journal of Endocrinology. 2007; 192(1):261–267. https://doi.org/10.1677/joe.1.07059 PMID: 17210763

50. Pereira RC, Juppner H, Azucena-Serrano CE, Yadin O, Salusky IB, Wesseling-Perry K. Patterns of FGF-23, DMP1, and MEPE Expression in Patients with Chronic Kidney Disease. Bone. 2009; 45(6):1161–1168. https://doi.org/10.1016/j.bone.2009.08.008 PMID: 19679205

51. Courbebaisse M, Lanske B. Biology of Fibroblast Growth Factor 23: From Physiology to Pathology. Cold Spring Harbor Perspectives in Medicine. 2018; 8(5):a031260. https://doi.org/10.1101/cshperspect.a031260 PMID: 28778965

52. Dobolyi A, Dimitrov E, Palkovits M, Usdin T. The Neuroendocrine Functions of the Parathyroid Hormone 2 Receptor. Frontiers in Endocrinology. 2012; 3. https://doi.org/10.3389/fendo.2012.00121 PMID: 23060860

53. Schmitt P, Veldhuis D. PTH Secretion Patterns in Patients with Secondary Hyperparathyroidism. 1998; p. 13.